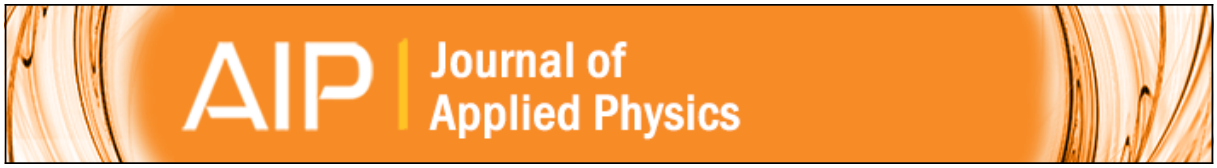

Optical constants of evaporation-deposited silicon monoxide films in the 7.1–800 eV photon energy range

Mónica Fernández-Perea, Manuela Vidal-Dasilva, Juan I. Larruquert, José A. Aznárez, José A. Méndez, Eric Gullikson, Andy Aquila, and Regina Soufli

Citation: Journal of Applied Physics **105**, 113505 (2009); doi: 10.1063/1.3123768
View online: http://dx.doi.org/10.1063/1.3123768
View Table of Contents: http://scitation.aip.org/content/aip/journal/jap/105/11?ver=pdfcov
Published by the AIP Publishing

Optical constants of evaporation-deposited silicon monoxide films in the 7.1–800 eV photon energy range

Mónica Fernández-Perea,[1,a)] Manuela Vidal-Dasilva,[1] Juan I. Larruquert,[1,b)] José A. Aznárez,[1] José A. Méndez,[1] Eric Gullikson,[2] Andy Aquila,[2] and Regina Soufli[3]
[1]*Instituto de Física Aplicada-Consejo Superior de Investigaciones Científicas, C/Serrano 144, 28006 Madrid, Spain*
[2]*Center for X-ray Optics, Lawrence Berkeley National Laboratory, Berkeley, California 94720, USA*
[3]*Lawrence Livermore National Laboratory, Livermore, California 94550, USA*

(Received 12 February 2009; accepted 22 March 2009; published online 2 June 2009)

The transmittance of silicon monoxide films prepared by thermal evaporation was measured from 7.1 to 800 eV and used to determine the optical constants of the material. SiO films deposited onto C-coated microgrids in ultrahigh vacuum conditions were measured *in situ* from 7.1 to 23.1 eV. Grid-supported SiO films deposited in high vacuum conditions were characterized *ex situ* from 28.5 to 800 eV. At each photon energy, transmittance, and thickness data were used to calculate the extinction coefficient k. The obtained k values combined with data from the literature, and with interpolations and extrapolations in the rest of the electromagnetic spectrum provided a complete set of k values that was used in a Kramers–Kronig analysis to obtain the real part of the index of refraction, n. Two different sum-rule tests were performed that indicated good consistency of the data. © *2009 American Institute of Physics*. [DOI: 10.1063/1.3123768]

I. INTRODUCTION

Silicon monoxide films have been widely used as protective layers,[1] antireflecting layers,[2] and multilayer spacers[3] in coatings for the visible and infrared spectral ranges and also as a replica and support material in the preparation of samples for electron microscopy.[4] In spite of the wide range of optical applications, the optical constants (n and k, with $\mathcal{N}=n+ik$ the complex index of refraction of the material) of SiO films have not been determined in most of the extreme ultraviolet (EUV) (~12–250 eV) and soft x rays (SXR) (~250 eV to several keV) spectral regions.

From previous work on the optical properties of SiO,[5] it is known that this material is more transparent than SiO_2 in the spectral region from 11 to 25 eV. On the other hand, it is less transparent than SiO_2 in the near UV and visible intervals. Additionally, its low vapor pressure when compared to Si or SiO_2 makes SiO films deposited onto room temperature substrates more uniform and adherent than their Si or SiO_2 counterparts.[6] Therefore, SiO thin films are expected to be suitable as protective layers for coatings in the spectral interval from 11 to 25 eV due to their relatively low absorption and good mechanical properties. A possible application of SiO protective layers in this interval would be their use as capping layers on lanthanide coatings. Lanthanides have been proposed recently as multilayer components for the EUV (Ref. 7) and their strong reactivity makes the use of a protective layer mandatory. The optical characterization of SiO films at EUV and SXR photon energies is also interesting from a theoretical point of view.

Philipp[5] obtained the dielectric function $\varepsilon=N^2$ of SiO films from ~1.5–26 eV by applying the Kramers–Kronig analysis to reflectance measurements performed from 1.5 to 25 eV. The author also obtained the absorption coefficient from transmittance measurements in the interval from 1.5 to 9 eV. These data were taken into account in order to carry out an adequate extrapolation of reflectance at energies larger than 25 eV. We have found that the extinction coefficient data calculated by using the absorption coefficient from Fig. 3 of Ref. 5 and the dielectric function from Fig. 5 of Ref. 5 are in disagreement for energies above ~5 eV. According to Philipp,[8] caution must be taken for energies above 12 eV because of the dependence of the dielectric function on the extrapolation of reflectance performed in Ref. 5. Reference 8 recommends to perform new measurements above 25 eV in order to improve the accuracy of the high-energy data of Ref. 5. Tarrio and Schnatterly[9] used inelastic electron scattering spectra to determine the absorption coefficient α of SiO films from 90 to 170 eV, the imaginary part of the dielectric function ε_2 from 2 to 20 eV and the absolute loss function $\mathrm{Im}(-1/\varepsilon)$ from 2 to 40 eV.

Outside the spectral region covered in the present work, Hass and Salzberg[1] determined the extinction coefficient k of SiO films in the spectral ranges from 0.089 to 0.155 eV and from 2.25 to 5.17 eV. The real part of the index of refraction n was calculated from 0.089 to 5.17 eV. The dependence of the films stoichiometry on the base pressure and deposition rate was also studied. It was found that both slow evaporation in high vacuum (HV) (base pressure ~10^{-4} Pa) and heating in air produced a deviation of the SiO stoichiometry so that the O-to-Si-atom ratio was higher than unity. The resulting SiO_x ($x>1$) films showed lower absorption in the UV and lower index of refraction in the whole studied spectral range than stoichiometric SiO films. Hjortsberg and Granqvist[10] reported dielectric function values in the spectral range from 0.0368 to 0.155 eV. Their results are in very good

a)Electronic mail: monicafp@ifa.cetef.csic.es.
b)Electronic mail: larruquert@ifa.cetef.csic.es. Tel.: +34 91 561 8806. FAX: +34 91 411 7651.

agreement with Ref. 1 in the overlapping region. López and Bernabéu[11] and Pérez *et al.*[3,12] determined the complex refractive index $\mathcal{N}$ from transmittance measurements of SiO films deposited at various substrate temperatures in the spectral range from 0.207 to 0.992 eV. Rawlings,[13] Hirose and Wada,[14] and Cremer *et al.*[15] reported the extinction coefficient k and the absorption coefficient $\alpha=4\pi k/\lambda$ of SiO films within the intervals of 1.46–2.76, 2.48–3.81and 2.07–4.96 eV, respectively. In all the aforementioned references SiO thin films were deposited by thermal evaporation in HV systems.

The goal of the present work is to obtain reliable SiO optical constants from transmittance measurements performed on thin films deposited by evaporation in HV or ultrahigh vacuum (UHV) conditions in the EUV and SXR spectral ranges, where most of the data are lacking or need to be revised. Section II describes the experimental techniques used in this work. Section III reports on the experimental results: the calculation of the extinction coefficient from the slope of transmittance versus thickness data and the Kramers–Kronig analysis that provides the real part of the index of refraction. Inertial and f sum rules provided a way to check the quality of both the real and imaginary parts of the obtained index of refraction.

II. EXPERIMENTAL TECHNIQUES

The extinction coefficient values presented below were derived from transmittance (T) measurements performed on samples with SiO thin films of different thicknesses. This method requires the use of transparent samples, which is accomplished by supporting the thin films on microgrids, as will be described below. T is calculated as the ratio of the incident beam intensity to the transmitted (through the sample) beam intensity, and is related to SiO thickness (d) by the approximate relation

$$\ln(T) \approx A + (-4\pi k/\lambda) \times d, \tag{1}$$

where λ stands for the radiation wavelength and A is a constant that accounts for the substrate transmittance and for the reflectance at the vacuum-SiO interface. A native oxide or hydrocarbon layer which may be present on the surface of all the samples would also contribute as an additive constant to Eq. (1) and therefore would not interfere with the k determination. At each photon energy, a straight line was fitted to the experimental $\ln(T)$ versus d data by the method of least-squares. For Eq. (1) to be correct it is necessary that multiple reflections inside the SiO film be negligible, which can occur both if the absorption of the film is high and if the reflectivity at the film interfaces is low. It will be shown below that in the present case this condition is fulfilled.

Samples were prepared by means of thermal evaporation at the Grupo de Óptica de Láminas Delgadas (GOLD) at Instituto de Física Aplicada, Consejo Superior de Investigaciones Científicas (Spain). The measurements were split into two groups attending to the photon energy. Measurements from 7.1 to 23.1 eV were performed *in situ* in UHV conditions at GOLD. For energies above 28.5 eV the measurements were performed *ex situ* at beamline 6.3.2. of the Advanced Light Source (ALS) synchrotron, at Lawrence Berkeley National Laboratory, Berkeley, California (USA).

A. Transmittance measurements from 7.1 to 23.1 eV at GOLD

The experimental equipment at GOLD consists of a far and EUV (FUV-EUV) (with FUV ranging from about 6 to 12 eV) reflectometry chamber at UHV pressure attached to an UHV preparation chamber. Ion and Ti sublimation pumping systems provide a base pressure of 1×10^{-8} Pa after baking at 470 K. The chambers are connected in vacuum so that samples are maintained under UHV conditions from deposition to optical characterization. A complete description of the experimental equipment can be found elsewhere.[16]

SiO thin films with four different thicknesses were prepared through four successive thermal evaporations performed on the same area of a substrate. In this way, the subsequently added layers accumulate to form a new film with a thickness equal to the total deposited thickness. The transmittance of each film was measured immediately after each deposition. The time elapsed between two evaporations ranged from 24 to 72 h. In order to evaluate the possibility of contamination of the films surface during this time, reflectance measurements, which are very sensitive to surface contamination were performed before and after 7 days of storage in the UHV reflectometry chamber. Reflectance values remained unchanged within the uncertainty limits. This result was expected given the small partial pressure of oxidizing species inside of UHV chambers ($P_{H_2O}\approx2\times10^{-9}$ Pa, $P_{CO_2}\approx2\times10^{-9}$ Pa, and $P_{O_2}<10^{-10}$ Pa, according to quadrupole mass spectrometer measurements). We therefore conclude that the hypothetical contamination on the surface of the films during the preparation and characterization of the samples, if any, is undetectable in reflectance and transmittance measurements.

The evaporation source was a Ta boat. Pressure during evaporation ranged from 2×10^{-7} to 2×10^{-6} Pa, and deposition rate was maintained from 3 to 5 nm/min. We followed the recommendations of Ref. 6 regarding the temperature of the evaporation source, which must be maintained at about 1520 K in order to obtain stoichiometric SiO films. The electrical parameters which provided a source temperature of ~1520 K were calibrated with an optical pyrometer. The distance from the evaporation source to the substrate was 38 cm. SiO raw material was purchased from Cerac, Inc. and it had a nominal purity of 99.97%.

Thickness was controlled with a quartz-crystal monitor that had been previously calibrated by means of Tolansky[17] interferometry. After the depositions and transmittance measurements were completed, the total thickness, corresponding to the thickest film, was measured with the aforementioned interferometric technique on a glass witness. The witness was located close to the sample during depositions, and therefore it was coated with a thickness identical to that of the sample. Total thickness, corresponding to the thickest of the studied films was found to be 47.0 nm. The thickness of the other three films was determined to be 17.3, 27.2, and 37.1 nm. This was accomplished using the nominal thickness

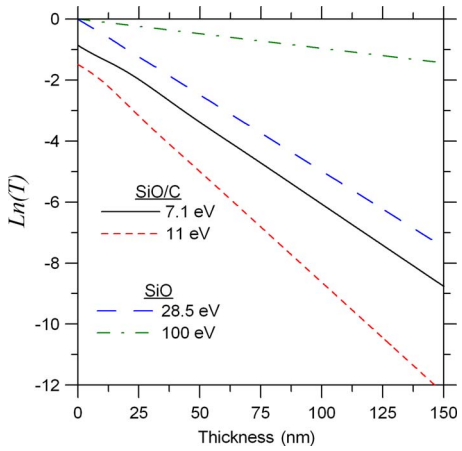

FIG. 1. (Color online) Calculated natural logarithm of the transmittance of SiO samples as a function of SiO film thickness for several photon energies. The effect of multiple reflections at the film interfaces has been included in the calculation.

ratio of each of the three films to the 47.0-nm-thick film, determined during the deposition process by the quartz-crystal monitor. The overall accuracy in film thickness determination with the above process is estimated to be 5%.

The substrate used for the four successively deposited films discussed above consisted of a Ni microgrid with a nominal open area of 88.6% on which a ~12-nm-thick C thin film had been deposited. We used a microgrid with squared holes of 203 μm per side separated by bars 12.7 μm thick. The thickness of the grid was 15 μm. The high transmittance of grid-supported thin-film substrates makes possible to perform transmittance measurements at FUV, EUV, and SXR wavelengths. C films were deposited by evaporation with an electron gun on the microgrid coated with a collodion film. The collodion was later dissolved in amyl acetate.

Equation (1) is a good approximation provided that multiple reflections inside the SiO film are negligible. The contribution of multiple reflections to the transmittance depends simultaneously on the reflectance at the SiO inner interfaces, the film absorption and the film thickness. In the case of absorbing materials such as SiO in the studied spectral region, Eq. (1) will be correct for thickness values larger than a threshold. The procedure to know whether Eq. (1) was applicable in our case consisted in plotting the experimental data of $\ln(T)$ versus d. We only used those thicknesses which gave linear dependencies between $\ln(T)$ and d. For photon energies below 11.8 eV the thinnest film (17.3 nm) did not comply with the linearity requirement so it was not used. At energies above 11.8 eV the transmittance of the thicker film was extremely low (<0.001) and therefore it was not used either. After the determination of the optical constants the validity of Eq. (1) was further verified by plotting calculated values of the $\ln(T)$ versus d. These calculated values were obtained with the usual equations based on Fresnel coefficients and therefore included the multiple reflections contribution. The result is shown in Fig. 1 for photon energies of 7.1 and 11 eV. The curves correspond to the transmittance of a SiO film on a 12-nm-thick C film as a function of SiO thickness calculated from the obtained optical constants (see Sec. III). We used C optical constants from a previous work.[18] The contribution of the Ni microgrid to the transmittance was not included in the calculation because it is a constant factor and therefore it does not influence the validity of Eq. (1). From the linearity range of the curves it is concluded that Eq. (1) is correct for the selected film thicknesses. The same is true for the rest of the 7.1–23.1 eV interval.

The EUV-FUV radiation source at GOLD is a windowless capillary discharge lamp connected to the reflectometer chamber through a differential pumping system that maintains a pressure gradient from about 100 Pa in the lamp exit to 1.5×10^{-7} Pa in the reflectometer during lamp operation. By using a quadrupole mass spectrometer it was seen that the main component of the residual atmosphere in the reflectometer is the nonoxidizing gas mixture flowing through the discharge lamp.

B. Transmittance measurements from 28.5 to 800 eV at 6.3.2 beamline

Samples consisted of SiO thin films of five different thicknesses supported on Ni microgrids similar to those described in Sec. II A. SiO deposition was performed at GOLD, in a HV system with a turbomolecular pumping and a base pressure of 8×10^{-5} Pa. The samples were prepared with the same technique that was used to prepare the C substrate in Sec. II A: SiO films were condensed onto collodion-coated Ni microgrids and the collodion was later dissolved in amyl acetate. SiO raw material was purchased from Balzers and it had a nominal purity of 99.8%. The distance from the evaporation source (Ta boat) to the substrate was 30 cm. Evaporation rate was maintained at about 6 nm/min, corresponding to a source temperature of about 1520 K. Thickness was controlled with a quartz-crystal monitor and measured by means of Tolansky[17] interferometry. The thickness measurement was performed after venting the deposition chamber, on a witness sample deposited on a glass substrate. The individual film thicknesses were thus determined to be 19.4, 39.7, 58.4, 118.0, and 160.5 nm.

Regarding the validity of Eq. (1), experimental $\ln(T)$ versus d plots showed a good linearity for all of the above thicknesses and the spectral range from 28.5 to 800 eV. Figure 1 shows the exact calculation of the transmittance of a self-supported SiO film for photon energies of 28.5 and 100 eV as a function of SiO film thickness, where we used SiO optical constants determined in this work (Sec. III). The contribution of the Ni microgrid to the transmittance was not included. From the linearity range of the curves it is concluded that Eq. (1) is correct for the selected film thicknesses. The same is applicable to the rest of the 28.5–800 eV interval. Transmittance measurements were performed after ~1 month of exposure to the atmosphere.

We also determined the SiO films density by weighing a piece of Al foil of known area before and after it was coated with a SiO film of known thickness. The resulting density value was $\rho_{SiO}=2.17\pm0.05$ g$\times$cm^{-3}, which is consistent both with the density value of bulk SiO ($\rho_{SiO}=2.15$ g$\times$cm^{-3}) and of thin film SiO ($\rho_{SiO}=2.18$ g$\times$cm^{-3}) from the literature.[6]

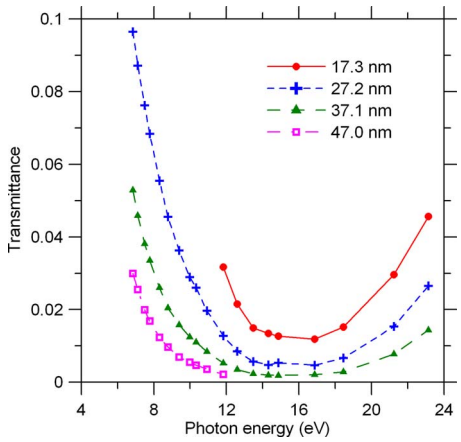

FIG. 2. (Color online) The transmittance of SiO films deposited onto a grid-supported C thin-film substrate is plotted as a function of photon energy from 7.1 to 23.1 eV. Measurements were performed *in situ* at GOLD, CSIC. The thickness of each film is indicated.

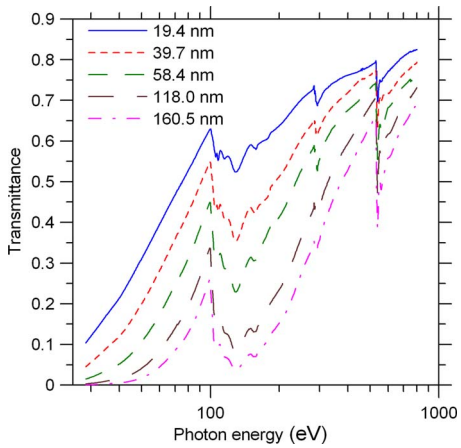

FIG. 3. (Color online) The transmittance of grid-supported SiO films is plotted as a function of photon energy (log scale) from 28.5 to 800 eV. Measurements were performed *ex situ* at beamline 6.3.2, ALS synchrotron, LBNL. The thickness of each film is indicated.

The characteristics of the ALS beamline 6.3.2 and its measurement chamber have been described in detail earlier.[19,20] A variable-spacing grating monochromator utilizing 80-, 200-, 600-, and 1200-line/mm gratings was used to access photon energies from 28.5 to 800 eV. The monochromator exit slit was set to a width of 50 μm for all transmittance measurements. Depending on the photon energy and grating used, the spectral resolving power varied from 300 to 3500 across the 28.5–800 eV region. Energy was calibrated based on absorption edges of filters installed at the beamline, with a relative accuracy of 0.04%–0.011% rms (depending on photon energy) and with 0.007%–0.05% repeatability. Second-harmonic and stray-light suppression at various energies were achieved with a selection of filters installed at the beamline. At low energies, where higher harmonics are present, an order suppressor consisting of three grazing-incidence mirrors was used in addition to filters. Any residual broadband scattered light from the beamline is suppressed with use of trimming slits located just upstream of the reflectometer. In this way, a spectral purity of 99.9% or better is achieved throughout the beamline spectral range. The ALS storage-ring current was used to normalize the signal against the storage-ring current decay. The base pressure in the measurement chamber was 10^{-4} Pa. The signal was collected on a Si photodiode detector with a 10×10 mm^2 active area and acceptance angle of 2.4°. The size of the beam spot (50×300 μm^2 full width at half maximum) and the Ni microgrid holes were comparable, therefore a precise positioning of the sample was necessary in order to obtain a maximum signal both for the direct and transmitted beams.

III. RESULTS AND DISCUSSION

A. Transmittance and extinction coefficient data

Transmittance measurements in the photon energy range from 7.1 to 23.1 eV are shown in Fig. 2, for the samples discussed in Sec. II A. The highest absorption observed at about 16 eV is due to a combination of SiO absorption and the peak absorption of C at about 15 eV.[21] The transmittance of the samples discussed in Sec. II B from 28.5 to 800 eV is displayed in Fig. 3. There are dips in transmittance associated with the Si $L_{2,3}$ absorption edge at 99.8 and 99.4 eV and the O K absorption edge at 543.1 eV.[22] The C K absorption edge at 284.2 eV indicates the presence of carbon on the surface of the samples. The transmittance plotted in Figs. 2 and 3 is reduced by a constant factor (11.4%) due to the presence of the microgrid.

The SiO extinction coefficient was determined from the slope of $\ln(T)$ versus d using Eq. (1). This method eliminates the contribution of the microgrid and of any native oxide or hydrocarbon layers which may be present in the surface of the SiO films, provided that the thickness of such layers is the same on all samples. Figure 4 shows the calculated extinction coefficient data[23] in the covered spectral range. The complete absence of the C K edge at 284.2 eV suggests that the carbon-related contamination observed in the transmission data in Fig. 3 indeed existed in the form of an overlayer of equal thickness among all the samples characterized *ex situ*, and was thus normalized out in the results in Fig. 4. Figure 4 also displays data from the literature. At low energies we have plotted the two sets of extinction coefficient

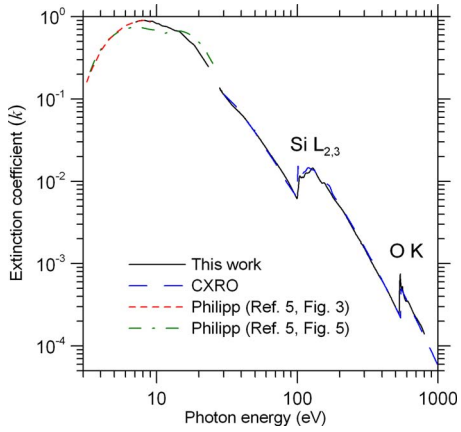

FIG. 4. (Color online) Log-log plot of the extinction coefficient of SiO films vs photon energy. Experimental values from Philipp (Ref. 5) are also displayed. CXRO data (Ref. 24), which were calculated for a density value of $\rho_{SiO}=2.17$ g$\times$cm^{-3}, are also plotted.

values from Philipp (calculated from data of Figs. 3 and 5 of Ref. 5). As mentioned before, the two sets are very similar for photon energies up to ~5 eV, but at higher energies we observe considerable differences. Data from this work are in very good agreement with k values from Fig. 3 of Ref. 5 in the overlapping region. At photon energies larger than 30 eV data downloaded from the CXRO web page[24] for SiO with a density $\rho_{SiO}=2.17\ \mathrm{g\times cm^{-3}}$ was also plotted on Fig. 4 of this work.

Reference 24 calculates the refractive index $\mathcal{N}$ of a compound from the atomic scattering factors of the constituent elements (f_j) in the independent-atom approximation,

$$\mathcal{N}=n+ik=1-\delta+ik=1-\frac{1}{2\pi}r_0\lambda^2\sum_j N_j^{\mathrm{at}}f_j, \tag{2}$$

where $\delta=1-n$, r_0 is the classical electron radius, λ is the wavelength of the radiation, and N_j^{at} are the atomic densities of the constituent elements. From the experimental density it is possible to obtain $N_{\mathrm{Si}}^{\mathrm{at}}$ and $N_{\mathrm{O}}^{\mathrm{at}}$ from

$$N_{\mathrm{Si}}^{\mathrm{at}}=N_{\mathrm{O}}^{\mathrm{at}}=\rho_{\mathrm{SiO}}/m_u(A_{\mathrm{Si}}+A_{\mathrm{O}}), \tag{3}$$

where m_u is the atomic mass unit and, A_{Si} and A_{O} are the atomic weights of Si and O, respectively. In the case of Si the atomic scattering factors come from experimental optical constants[25] for energies in the 30 to 500 eV interval, and from Henke *et al.*[26] in the rest of the spectrum. In the case of O the atomic scattering factors come entirely from Ref. 26. The independent-atom approximation is valid for photon energies larger than about 30 eV and sufficiently far from absorption edges. Figure 4 shows a good agreement between k data from this work and k data from CXRO except for photon energies close to the absorption edges.

The uncertainty in the determination of the extinction coefficient k was estimated in the following way: a computer code was used to simulate additional measurements by adding random errors to the experimental measurements; at every simulated measurement, transmittance and thickness values were randomly modified within the limits imposed by their relative uncertainties (estimated in ~2% in the case of transmittance and ~5% in the case of thickness). With these modified values, the extinction coefficient was calculated in the usual way through the slope of $\ln(T)$ versus thickness. After a large number of measurement simulations, the standard deviation σ_k of the resulting set of extinction coefficient values was interpreted as δk, the uncertainty of k, with k taking values within $k\pm\delta k$. As a result of this procedure the relative uncertainty $\delta k/k$ of the SiO extinction coefficient was determined to be between $\sim\pm1\%$ and $\pm4\%$ in the whole studied spectral range.

Figures 5 and 6 show in more detail the extinction coefficient near the Si $L_{2,3}$ and O K absorption edges, along with values from the literature. k values at both edges differ substantially from CXRO data because the independent-atom approximation is not valid in the vicinity of the absorption edges. The onset of the O K edge for SiO in Fig. 6 has shifted to lower energy compared to elemental O (543.1 eV) and is located at about 532 eV, which is consistent with experimental x-ray photoelectron spectroscopy data on

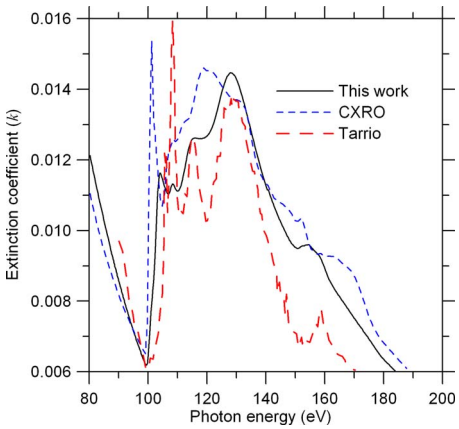

FIG. 5. (Color online) The extinction coefficient of SiO is plotted in the spectral region close to the Si $L_{2,3}$ absorption edge. Experimental values from Tarrio and Schnatterly (Ref. 9) are also displayed. CXRO data (Ref. 24) ($\rho_{SiO}=2.17\ \mathrm{g\times cm^{-3}}$) are also plotted.

evaporated SiO films published earlier in the literature.[27] Near-edge x-ray-absorption fine structure in the vicinity of the O K edge was also revealed in the present SiO measurements, as shown in Fig. 6. When compared to Tarrio and Schnatterly[9] data near the Si $L_{2,3}$ edge, the k values in the present manuscript exhibit substantially broader peaks, with the peaks located at similar photon energies.

B. Refractive-index calculation with the dispersion relations

In order to obtain a complete set of extinction coefficient values in the entire electromagnetic spectrum we gathered data from the literature in the following way: Hjortsberg and Granqvist[10] extinction coefficient values were used from 0.0368 to 0.089 eV. These data connected smoothly with k values from Hass and Salzberg,[1] which were used up to 0.155 eV. From Pérez and Sanz[12] we obtained k values in the interval 0.42−0.992 eV. Considering that extinction coefficient values from Philipp[5] in Fig. 3 are in good agreement with ours in the overlapping region, we used these values in the interval 1.5–7.1 eV instead of data coming from Philipp[5] in Fig. 5. k data downloaded from the CXRO web page,[24]

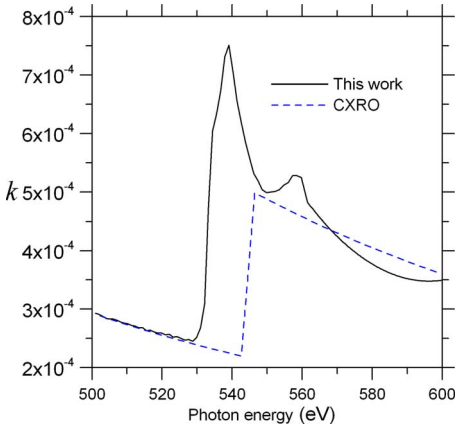

FIG. 6. (Color online) The extinction coefficient (log scale) of SiO is plotted in the spectral region close to the O K absorption edge. CXRO data (Ref. 24) ($\rho_{SiO}=2.17\ \mathrm{g\times cm^{-3}}$) are also plotted.

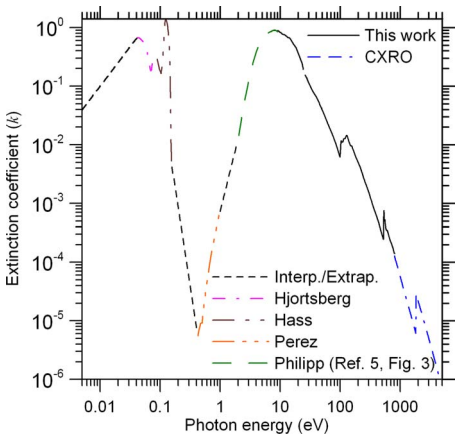

FIG. 7. (Color online) Log-log plot of the extinction coefficient data set used in the Kramers–Kronig analysis. Data from Hjortsberg and Granqvist (Ref. 10), Hass and Salzberg (Ref. 1), Pérez and Sanz (Ref. 12) and Philipp (Ref. 5) were used along with data from this work. CXRO data (Ref. 24) ($\rho_{SiO}=2.17\ \mathrm{g\times cm^{-3}}$) were used from 8×10^2 to 3×10^4 eV.

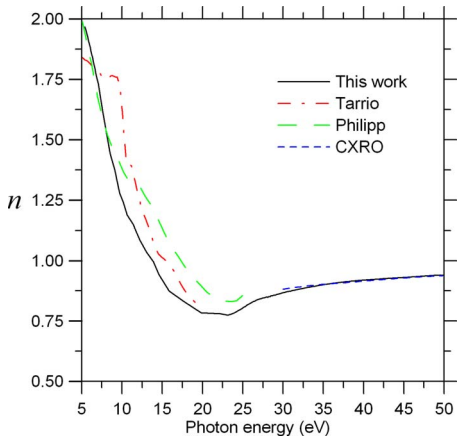

FIG. 8. (Color online) The real part of the index of refraction is shown in the low-energy portion of the studied spectral range. Experimental values from Tarrio and Schnatterly (Ref. 9) and Phillip (Ref. 5) are also displayed. CXRO data (Ref. 24) ($\rho_{SiO}=2.17\ \mathrm{g\times cm^{-3}}$) are also plotted for energies larger than 30 eV.

which were calculated with the experimentally determined density, were used from 800 eV up to 3×10^4 eV. The gaps from 0.155 to 0.42, 0.992 to 1.5, and 23.1 to 28.5 eV were filled by using smooth interpolations. An extrapolation to zero energy was performed by fitting the low-energy data from Ref. 10 to the function $k=k_0(E/E_0)^\beta$, with $\beta=1.348$. $k_0=0.579$ is the extinction coefficient value at a photon energy $E_0=0.0368$ eV, which is the smallest photon energy where there are available k values in the literature. Another extrapolation was performed at energies higher than 3×10^4 eV in which we maintained constant the slope of data from Ref. 24. This assumption resulted in a function of the form $k=k_0(E/E_0)^\beta$ with $\beta=-3.880$, $k_0=6.699\times10^{-10}$ and $E_0=3\times10^4$ eV, the highest photon energy were there are available values in the literature. The obtained complete set of extinction coefficient data is displayed in Fig. 7.

The consistency of the k data set has been evaluated by means of the f-sum rule,[28] which may be written in the following form:

$$n_{\mathrm{eff}}(E)=\frac{4\varepsilon_0 m}{\pi N_{\mathrm{SiO}} e^2 h^2}\int_0^E E'k(E')dE'. \tag{4}$$

This equation provides the number of electrons per molecule contributing to SiO absorption up to a photon energy E. ε_0 stands for the permittivity of vacuum, m is the electron mass, h is Planck's constant, and N_{SiO} is the number of SiO molecules per unit volume. The limit of n_{eff} at high energies must converge to the total number of electrons of the SiO molecule, which is $Z_{\mathrm{SiO}}=Z_{\mathrm{Si}}+Z_{\mathrm{O}}=22$. The limit calculated with Eq. (4) is 21.43, which is only 2.6% lower than the expected value. We conclude that the f-sum rule test, evaluated with the complete set of k values, results in a satisfactory value.

The complete set of extinction coefficient data was used to calculate the real part of the index of refraction of SiO films by means of the Kramers–Kronig relation

$$n(E)-1=\frac{2}{\pi}P\int_0^\infty \frac{E'k(E')}{E'^2-E^2}dE', \tag{5}$$

where P stands for the Cauchy principal value. Note that in order to obtain n at a single photon energy it is necessary to know the extinction coefficient of the material in the whole electromagnetic spectrum.

Figure 8 displays the calculated n values[23] from 5 to 50 eV, along with data from the literature. At energies lower than ~8 eV present data match well Philipp's data, which were calculated from the dielectric function displayed in Fig. 5 of Ref. 5. On the other hand, there are differences above ~8 eV. This result is in agreement with comments in Ref. 8 about data in Ref. 5, regarding the convenience of performing new measurements above 25 eV in order to improve the accuracy of the high-energy data of Ref. 5. Tarrio and Schnatterly[9] data do not match either current data or Philipp's. At higher energies, CXRO data are very similar to present data.

Figure 9 shows the calculated δ values from about 14 to 800 eV along with CXRO data. A good coincidence is ob-

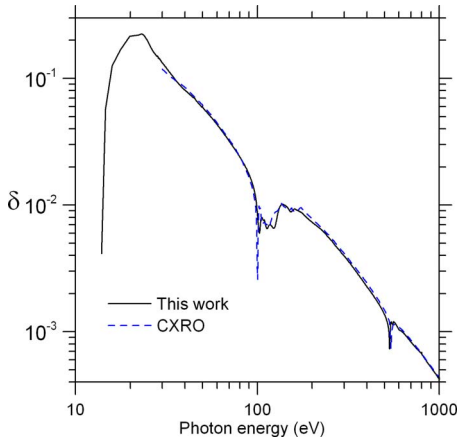

FIG. 9. (Color online) $\delta=1-n$ of SiO is plotted in log-log scale in the high-energy portion of the studied range. CXRO data (Ref. 24) ($\rho_{SiO}=2.17\ \mathrm{g\times cm^{-3}}$) are also plotted for energies larger than 30 eV.

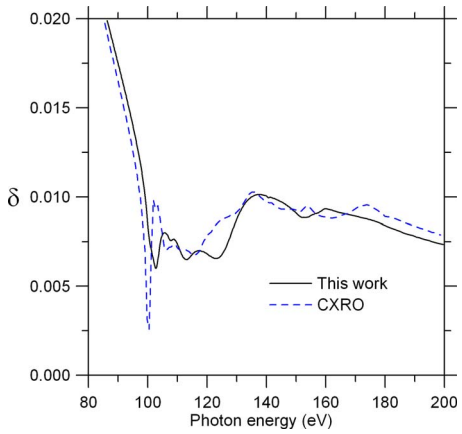

FIG. 10. (Color online) δ of SiO films is plotted in the spectral region close to the Si $L_{2,3}$ absorption edge. CXRO data (Ref. 24) ($\rho_{SiO}=2.17$ g$\times$cm^{-3}) are also plotted.

served except for photon energies close to the absorption edges, which are plotted in detail in Figs. 10 and 11.

The evaluation of the consistency of n data was performed by means of the inertial-sum rule,

$$\int_0^\infty [n(E)-1]dE = 0, \tag{6}$$

which expresses that the average of the refractive index throughout the spectrum is unity. The following parameter is defined to evaluate how close to zero the integral of Eq. (6) (Ref. 28) is

$$\zeta = \frac{\int_0^\infty [n(E)-1]dE}{\int_0^\infty |n(E)-1|dE}. \tag{7}$$

Shiles *et al.*[28] suggested that a good value of ζ should stand within ± 0.005. We obtained an evaluation parameter of -0.0008, well within the aforementioned limit, which supports the consistency of the obtained real part of the index of refraction.

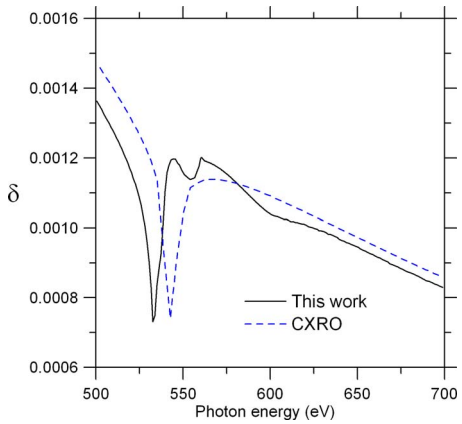

FIG. 11. (Color online) δ of SiO films is plotted in the spectral region close to the O K absorption edge. CXRO data (Ref. 24) ($\rho_{SiO}=2.17$ g$\times$cm^{-3}) are also plotted.

IV. CONCLUSIONS

Optical constants of evaporated SiO films have been obtained from transmittance measurements in the spectral range from 7.1 to 800 eV, where most of the data either were lacking or needed to be revised. The extinction coefficient (k) was determined directly from transmittance measurements. The Kramers–Kronig analysis provided a way to calculate the real part of the index of refraction (n). The extinction coefficient was first obtained from transmittance measurements for energies above 10 eV. We believe our data to be more consistent than previous experimental data available in the literature[5] in the spectral range from 10 to 25 eV, as we performed measurements over a wider spectral range extended to much higher energies. As far as we know, the real part of the index of refraction was experimentally determined for the first time at energies higher than 28.5 eV. We checked the consistency of the optical constants with both f- and inertial-sum rules. The relative transparency of SiO at EUV wavelengths compared to other stable materials along with its capability of forming thin uniform layers, make this material very promising as a protection layer for lanthanide multilayers working at the EUV.

ACKNOWLEDGMENTS

This work was supported by the National Programme for Space Research, Subdirección General de Proyectos de Investigación, Ministerio de Ciencia y Tecnología, Project Nos. ESP2002-01391 and ESP2005-02650. This work was also performed under the auspices of the U.S. Department of Energy by the University of California Lawrence Berkeley National Laboratory under Contract No. DE-AC03-76F00098 and by the University of California Lawrence Livermore National Laboratory under Contract No. DE-AC52-07NA27344. M.F.-P. is thankful to Consejo Superior de Investigaciones Científicas (Spain) for funding under the Programa I3P (Contract No. I3P-BPD2004), partially supported by the European Social Fund. M.V.-D. acknowledges financial support from a FPI Contract No. BES-2006-14047 fellowship. We acknowledge the technical assistance of José M. Sánchez-Orejuela.

[1] G. Hass and C. D. Salzberg, J. Opt. Soc. Am. **44**, 181 (1954).
[2] G. Hass, H. H. Schroeder, and A. F. Turner, J. Opt. Soc. Am. **46**, 31 (1956).
[3] G. Pérez, A. M. Bernal-Oliva, E. Márquez, J. M. Gónzalez-Leal, C. Morant, I. Génova, J. F. Trigo, and J. M. Sanz, Thin Solid Films **485**, 274 (2005).
[4] D. E. Bradley, in *Techniques for Electron Microscopy*, edited by D. Kay (Blackwell Scientific Publications, Oxford, 1961), Chap. 3.
[5] H. R. Philipp, J. Phys. Chem. Solids **32**, 1935 (1971).
[6] G. Hass, J. Am. Ceram. Soc. **33**, 353 (1950).
[7] M. Fernández-Perea, M. Vidal-Dasilva, J. A. Aznárez, J. I. Larruquert, J. A. Méndez, L. Poletto, D. Garoli, A. M. Malvezzi, A. Giglia, and S. Nannarone, J. Appl. Phys. **104**, 123527 (2008) (and references therein).
[8] H. R. Philipp, in *Handbook of Optical Constants of Solids*, edited by E. D. Palik (Academic, New York, 1985), pp. 765–769.
[9] C. Tarrio and S. E. Schnatterly, J. Opt. Soc. Am. B **10**, 952 (1993).
[10] A. Hjortsberg and C. G. Granqvist, Appl. Opt. **19**, 1694 (1980).
[11] F. López and E. Bernabéu, Thin Solid Films **191**, 13 (1990).
[12] G. Pérez and J. M. Sanz, Thin Solid Films **416**, 24 (2002).
[13] I. R. Rawlings, Br. J. Appl. Phys. **1**, 733 (1968).
[14] H. Hirose and Y. Wada, Jpn. J. Appl. Phys., Part 1 **3**, 179 (1964).
[15] E. Cremer, Th. Graus, and E. Ritter, Z. Elektrochem. **62**, 939 (1958).

[16]J. A. Aznárez, J. I. Larruquert, and J. A. Méndez, Rev. Sci. Instrum. **67**, 497 (1996).
[17]S. Tolansky, *Multiple-Beam Interferometry of Surfaces and Films* (Oxford University Press, London, 1948).
[18]M. Fernández-Perea, J. A. Aznárez, J. I. Larruquert, J. A. Méndez, L. Poletto, D. Garoli, A. M. Malvezzi, A. Giglia, and S. Nannarone, J. Appl. Phys. **103**, 073501 (2008).
[19]J. H. Underwood and E. M. Gullikson, J. Electron Spectrosc. Relat. Phenom. **92**, 265 (1998).
[20]E. M. Gullikson, S. Mrowka, and B. B. Kaufmann, Proc. SPIE **4343**, 363 (2001).
[21]D. L. Windt, W. C. Cash, Jr., M. Scott, P. Arendt, B. Newnam, R. F. Fisher, A. B. Swartzlander, P. Z. Takacs, and J. M. Pinneo, Appl. Opt. **27**, 279 (1988).
[22]*Photoemission in Solids I: General Principles*, edited by M. Cardona and L. Ley (Springer-Verlag, Berlin, 1978); G. P. Williams, in *X-Ray Data Booklet*, edited by A. C. Thompson and D. Vaughan (Lawrence Berkeley Laboratory, Berkeley, 1986).
[23]See EPAPS Document No. E-JAPIAU-105-057909 for tabulated values of k, n and δ as a function of photon energy. For more information on EPAPS, see http://www.aip.org/pubservs/epaps.html.
[24]E. M. Gullikson, "X-ray interactions with matter," http://www-cxro.lbl.gov/optical_constants.
[25]R. Soufli and E. M. Gullikson, Appl. Opt. **36**, 5499 (1997).
[26]B. L. Henke, E. M. Gullikson, and J. C. Davis, At. Data Nucl. Data Tables **54**, 181 (1993).
[27]T. P. Nguyen and S. Lefrant, J. Phys.: Condens. Matter **1**, 5197 (1989).
[28]E. Shiles, T. Sasaki, M. Inokuti, and D. Y. Smith, Phys. Rev. B **22**, 1612 (1980).